




# Arteriolosclerosis differs from venular collagenosis in relation to cerebrovascular parenchymal damages: an autopsy-based study

Yuan Cao <sup>1</sup>, Mei-Ying Huang <sup>1</sup>, Chen-Hui Mao,<sup>1</sup> Xue Wang,<sup>2</sup> Yuan-Yuan Xu,<sup>2</sup> Xiao-Jing Qian,<sup>2</sup> Chao Ma,<sup>2</sup> Wen-Ying Qiu,<sup>2</sup> Yi-Cheng Zhu <sup>1</sup>

**To cite:** Cao Y, Huang M-Y, Mao C-H, *et al.* Arteriolosclerosis differs from venular collagenosis in relation to cerebrovascular parenchymal damages: an autopsy-based study. *Stroke & Vascular Neurology* 2023;**8**: e001924. doi:10.1136/svn-2022-001924

► Additional supplemental material is published online only. To view, please visit the journal online (<http://dx.doi.org/10.1136/svn-2022-001924>).

YC and M-YH contributed equally.  
W-YQ and Y-CZ contributed equally.

YC and M-YH are joint first authors.

Received 8 August 2022  
Accepted 11 December 2022  
Published Online First  
29 December 2022



© Author(s) (or their employer(s)) 2023. Re-use permitted under CC BY-NC. No commercial re-use. See rights and permissions. Published by BMJ.

For numbered affiliations see end of article.

**Correspondence to**  
Dr Yi-Cheng Zhu;  
zhuych910@163.com

## ABSTRACT

**Background and purpose** Cerebrovascular parenchymal damage is prevalent in ageing brains; however, its vascular aetiology has not been fully elucidated. In addition to the underlying role of sclerotic arterioles, the correlation between collagenised venules has not been clarified.

Here, we aimed to investigate the associations between microvascular injuries, including arteriolosclerosis and venular collagenosis, and related parenchymal damages in ageing brains, to investigate the underlying correlations.

**Methods** We evaluated arteriolosclerosis and venular collagenosis in 7 regions from 27 autopsy cases with no history of stroke or brain tumour. The correlations between the ratio of arteriolosclerosis, venular collagenosis and the severity of cerebrovascular parenchymal damage, including lacunes, microinfarcts, myelin loss, and parenchymal and perivascular haemosiderin deposits, were assessed.

**Results** Arteriolosclerosis and venular collagenosis became more evident with age. Arteriolosclerosis was associated with lacunes ( $p=0.004$ ) and brain parenchymal haemosiderin deposits in the superior frontal cortex ( $p=0.024$ ) but not with leukoaraiosis severity. Venular collagenosis was not associated with the number of lacunes or haemosiderin, while white matter generally became paler with severe venular collagenosis in the periventricular ( $\beta=-0.430$ ,  $p=0.028$ ) and deep white matter ( $\beta=-0.437$ ,  $p=0.025$ ).

**Conclusion** Our findings imply an important role for venular lesions in relation to microvessel-related parenchymal damage which is different from that for arteriolosclerosis. Different underlying mechanisms of both cerebral arterioles and venules require further investigation.

## INTRODUCTION

Cerebrovascular parenchymal damage, including lacunes, microinfarcts, myelin loss and haemosiderin deposits, is common during the autopsy of aged individuals.<sup>1,2</sup> Previous neuropathological studies have found that arteriolar sclerosis is closely correlated with brain tissue damage, indicating a potential aetiology of cerebrovascular parenchymal lesions.<sup>3</sup> Apart from the arteriolar injuries, histopathological studies also found that venular

### WHAT IS ALREADY KNOWN ON THIS TOPIC

⇒ Arteriolar sclerosis is closely correlated with brain tissue damage, while cerebral venules have been consistently ignored.

### WHAT THIS STUDY ADDS

⇒ We found an important role of venular lesions in microvessel-related parenchymal damage which is different from that of arteriolosclerosis.

### HOW THIS STUDY MIGHT AFFECT RESEARCH, PRACTICE OR POLICY

⇒ This finding may give a novel perspective in understanding of mechanism underlying microvessel-related parenchymal damage.

collagenosis, involving small veins and venules in periventricular regions, was associated with more severe myelin loss.<sup>4,5</sup> In addition, studies on brain venules have reported that it is sometimes possible to confuse abnormal venules with hyalinised arterioles without special stains.<sup>6</sup> Putting these findings together, questions on the roles and heterogeneities of arteriolar and venular abnormalities in the etiopathogenesis of parenchymal damage may be raised.

However, no pathological study has compared the roles of arteriolosclerosis and venular collagenosis in parenchymal damage. This may be largely due to the lack of specific staining methods to distinguish venules from arterioles, especially those with diameters of <1 mm. In view of the accumulating evidence on the role of the cerebral venous system relative to the glymphatic pathway, arterioles and venules should be comprehensively investigated to further understand the pathophysiological mechanisms of tissue damage caused by or associated with vessel disease.

To address these issues, we examined the topographical associations between

**Table 1** Clinicopathologic characteristics of 27 subjects

Characteristics	Total sample (n=27)
Age at death, mean±SD (years)	77.3±14.1
Male gender, n (%)	13 (48.2)
Case history	
Tumour, n (%)	11 (40.7)
Dementia, n (%)	7 (25.9)
Coronary heart disease, n (%)	1 (3.7)
Others, n (%)	7 (25.9)
Brain weight, mean±SD (g)	1139.2±111.6
Post-mortem delay, median IQR (hour)	8.4, 4.5–17
IOR, interquartile range; SD, standard deviation.	

cerebral microvascular injuries, including arteriolosclerosis and venular collagenosis, and different types of parenchymal damage associated with small vessel disease, including lacunes, microinfarcts, myelin loss, parenchymal haemosiderin deposits, and perivascular haemosiderin leakage in seven different cerebral regions from 27 postmortem cases, to explore the underlying pathophysiological mechanisms of different microvascular injuries.

## METHODS

### Specimen selection

Our study comprised 27 human postmortem brains (mean age: 77.33±14.07 years; 13 males), and the clinicopathological profiles are shown in [table 1](#) (details in online supplemental table 1). Cases with stroke or brain tumour history according to their clinical records (obtained at donation from the donors' family members, reviewed by W-YQ) were excluded from this study. Due to lack of detailed clinical records, vascular risk factors could not be accurately assessed for these cases. A more detailed description of the standardised protocol of the Human Brain Bank in China has been published elsewhere.<sup>7</sup> Written informed consent was obtained from both the brain donors and their next of kin.

The number of lacunes was recorded during the gross examination of the right hemisphere. After the autopsy, the right hemisphere was immersion-fixed in 10% buffered aqueous formaldehyde solution for 2–6 weeks, following which it was dissected in coronal planes at approximately 1.0 cm intervals and was paraffin-embedded. During brain autopsy, tissue blocks were systematically taken in all cases from the frontal periventricular white matter (the distance to the ependyma <0.5 cm), occipital periventricular white matter (the distance to ependyma <0.5 cm), deep white matter in the parietal lobe (the distance to ependyma >1.5 cm), superior frontal cortex (Brodmann area 9),

occipital cortex (Brodmann areas 17 and 18), hippocampus and putamen.

### HISTOLOGICAL PROCEDURES

Paraffin-embedded serial sections from seven tissue blocks were cut at a 5 µm thickness. Sections underwent histological staining with Luxol fast blue (LFB) to assess white matter pallor (as a measure of myelin loss), Prussian blue to demonstrate haemosiderin, Masson's trichrome to evaluate the degree of collagen deposition in the microvascular walls and H&E for visualising arteriole/venule walls, as well as microinfarcts in the brain parenchyma. Immunohistochemistry was performed using antibodies against alpha-smooth muscular actin (αSMA, Cat# 19245, RRID: AB\_2734735, rabbit monoclonal antibody, diluted 1:400; Cell Signaling Technology) and monocarboxylate transporter 1 (MCT1, Cat# 20139-1-AP, RRID: AB\_2878645, rabbit polyclonal antibody, diluted 1:800; Proteintech) to distinguish between venules and arterioles (details of primary antibodies and antigen retrieval protocols for immunohistochemistry are presented in online supplemental table 2).<sup>8</sup> Immunopositivity was detected using the VECTASTAIN ABC-HRP Kit (rabbit IgG, PK-4001; Vector Laboratories, Burlingame, California, USA) with 3,3 diaminobenzidine as a chromogen and hematoxylin as the counterstain. All histologically and immunohistochemically stained sections were subsequently dehydrated using a series of alcohols, cleared, and mounted in neutral balsam (ZLI-9555, ZSGB-BIO, Beijing, China).

### Image analysis

All image analyses were performed by two trained neurologists (YC and M-YH), who were blinded to the neuropathological diagnosis, and analysis results were re-examined and confirmed by one pathologist (W-YQ). Whole stained sections were scanned using an Aperio digital pathology slide scanner (Leica Biosystems), and monochrome images were uploaded into the Image J software programme (Media Cybernetics, USA; V.6.3).

### Assessing microvascular wall pathology

To evaluate the severity of arteriolosclerosis and venular collagenosis, 2400 µm×3800 µm single images were captured randomly in anti-αSMA and anti-MCT1 immunostained sections to differentiate arterioles and venules, and the corresponding visual fields on the delineated images were subsequently captured in the adjacent Masson's trichrome sections to assess the microvascular walls. Based on our previous report, arterioles were identified as negative immunolabeled for MCT1 and generally positive immunolabeled for αSMA.<sup>8</sup> According to the rating scheme for cerebrovascular lesions, arterioles with a score of 2 or 3 were assessed as arteriosclerotic arterioles in our study, following which the percentage of arteriolosclerosis was calculated.<sup>9</sup> Similarly, for venular

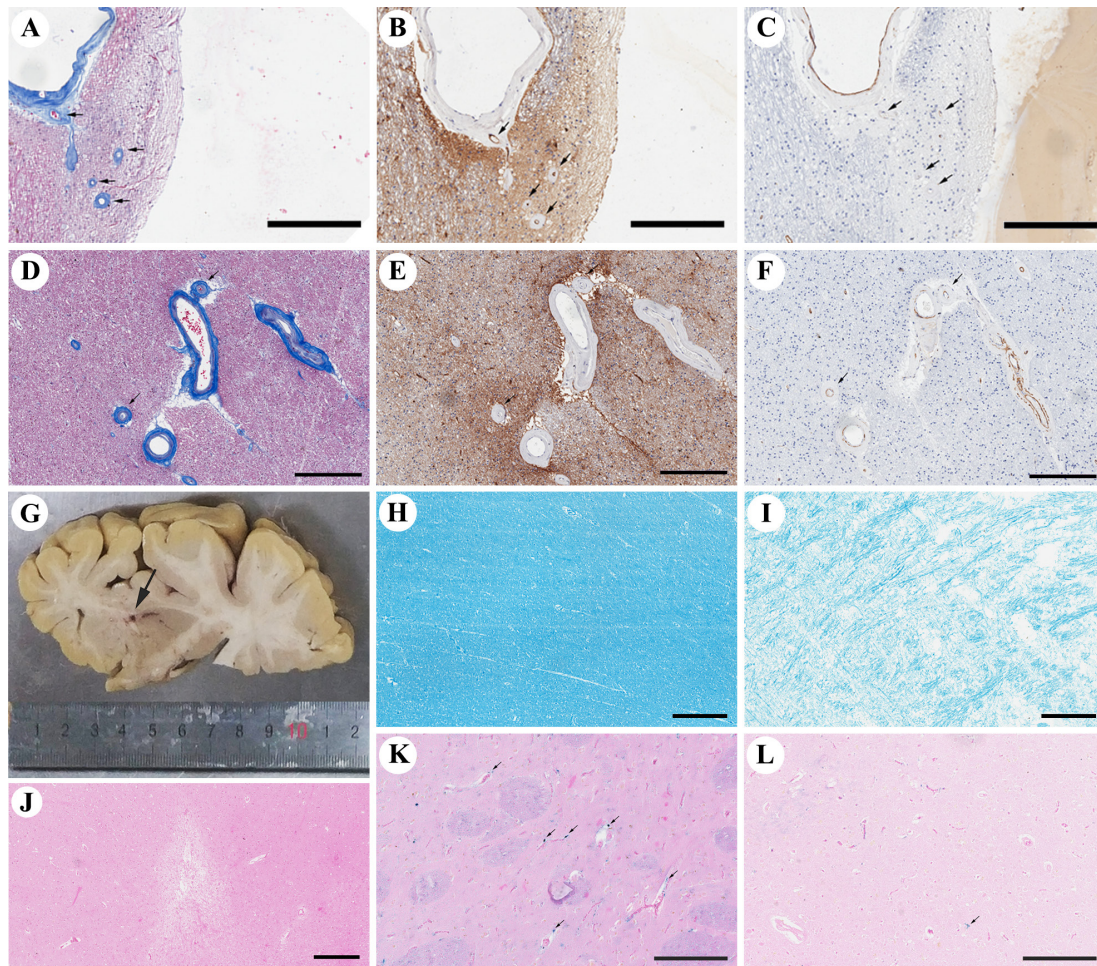


**Figure 1** Representative images of venular collagenosis, arteriolosclerosis and parenchymal damages. The venular collagenosis pathology is shown in (A) (black arrows, occipital periventricular white matter from patient 27), and images taken from consecutive sections show a venule pattern with anti-MCT1 immunopositivity in the endothelium (B) and pale anti- $\alpha$ SMA immunoreactivity in the media tunica (C). Arteriolosclerosis is shown in (D–F) (black arrows, frontal periventricular white matter from patient 27), with negative immunoreactivity of anti-MCT1. (G) Shows lacunes grossly (Patient 17). The value of LFB in H is 134.119 (deep white matter from patient 16), and that in I is 101.253 (frontal periventricular white matter from patient 17), indicating the severity of myelin loss. (J) Shows a microinfarct in the superior frontal cortex of Patient 11. Both (K, L) show Perls Prussian blue staining, with perivascular haemosiderin leakage shown in K (black arrows, putamen from patient 11) and parenchymal haemosiderin deposits shown in (L) (the black arrow, occipital cortex from patient 18). Bar=300  $\mu$ m for A–F and H–K, bar=500  $\mu$ m for J, and bar=200  $\mu$ m for (K, L).  $\alpha$ SMA, alpha-smooth muscular actin; LFB, Luxol fast blue.

collagenosis evaluation, vessels ranging from 10 to 300  $\mu$ m in diameter, which showed intense labelling for MCT1 in the endothelium with a thin anti- $\alpha$ SMA-stained pattern in the media tunica, were considered as venules,<sup>8</sup> and those with severe stenosis (the lumen occupying more than 50% of the vessel diameter) or occlusion by thick collagenous walls were assessed as venular collagenosis (figure 1) according to previous scores by Moody *et al.*<sup>4</sup> The ratio of the number of collagenised venules to the total number of venules in the visual field was calculated and expressed as a percentage of venular collagenosis.

#### Assessing and quantifying vascular parenchymal damages

Microinfarcts were identified as sharply delimited microscopic regions of cellular death or tissue necrosis, sometimes with cavitation (ie, a central fluid-filled cavity).<sup>2</sup> For the quantification of myelin loss, the 8-bit grayscale

threshold was manually adjusted to select only white matter regions. At each LFB-stained section, five images (1 mm  $\times$  1 mm) were captured randomly, and the inverted mean grey values of the LFB stain were measured using the Image J software. If necessary, the selected images were subjected to the manual setting of the regions of interest to exclude grey matter and meningeal structures. A pixel value of 0 represented white, and 255 represented black; therefore, a lower value signified a more severe white matter pallor, indicating myelin loss. The mean grey value was recorded for each of the five visual fields, and the mean value was calculated as the severity of myelin loss in the respective white matter region. To support the data accuracy by LFB stain, we also conducted anti-myelin basic protein (Cat# ab40390, RRID: AB\_1141521, rabbit polyclonal antibody, diluted

1:500; Abcam) immunohistochemistry stain in the adjacent sections, and assessed the images in a similar way (online supplemental figure 1). For haemosiderin evaluations, perivascular and brain parenchymal haemosiderin were assessed separately based on H&E-stained and Prussian blue-stained sections. For each selected region, the number of vessels with perivascular haemosiderin leakage on the entire slide was recorded, and the average number of haemosiderin deposits in the brain parenchyma was calculated from five 2 mm × 2 mm images.

### Statistics

Variables were tested for normality using the Shapiro-Wilk test and visual inspection of variable histograms. Descriptive analyses were conducted using the median and 25%–75% percentiles for continuous variables and frequency and percentage for categorical variables. Comparisons of cerebral small vessel pathology in different brain regions were conducted using the Wilcoxon matched-pairs signed-rank test. Spearman's correlation coefficients were used in the respective regions to investigate the association between the percentage of venular collagenosis or arteriolosclerosis and age. The Mann-Whitney U test for non-parametric analysis of the age was performed between patients with or without lacunes, and there was no significant difference in the age at death between groups (76.56±14.61 years for those with lacunes vs 76.44±14.66 years for those without lacunes,  $p=1.000$ ; 72.67±13.09 years for those with microinfarcts vs 79.67±14.31 years for those without microinfarcts,  $p=0.2088$ ). The Mann-Whitney U test was used for non-parametric analysis between patients with and without lacunes to compare the percentage of arteriolosclerosis or venular collagenosis in each region. Spearman's partial correlation coefficients (adjusted for age) were used to assess associations between these microvascular lesions and the number of microinfarcts, the mean grey value of LFB, and the number of haemosiderin deposits in each region. The significance level was set at 0.05, and all tests of significance were two tailed. All statistical analyses were conducted using SAS V.9.4 (SAS Institute).

### RESULTS

The characteristics of the 27 participants are presented in [table 1](#). The average age at death was 77.3 years (SD: 14.1 years), and 48.7% (13/27) of the donors were males. The median postmortem delay was 8.4 hours (IQR: 4.5–17 hours).

#### Parenchymal damages and microvascular wall pathology in different brain regions

Cerebrovascular parenchymal damage was evaluated across all selected white matter and grey matter regions, except for myelin loss, which was assessed only in the white matter ([figure 2](#)). In gross specimens, lacunes were observed in 59.26% (16/27) of the brains, and microinfarcts were observed under a microscope in 66.67%

(18/27) of the brains. The values of white matter pallor were lower in the periventricular white matter than that in the deep white matter (117.0±7.2 vs 119.1±7.5,  $p=0.05$ ), indicating a higher degree of myelin loss. Both parenchymal haemosiderin deposits and vessels with perivascular haemosiderin leakage were commonly observed in the putamen (median: 27.4 (parenchymal) and 15 (perivascular)) and were evenly distributed in all other regions (median range: 4.2–5.8 (parenchymal) and 0–1 (perivascular)).

Cerebral microvascular wall pathology was also observed in all brain regions ([figure 2](#)). In most brain areas, arteriolosclerosis and venular collagenosis were found in a similar distribution pattern, both of which were most frequently observed in the periventricular white matter, less so in the deep white matter and cortical grey matter, and least frequently observed in the hippocampus. However, in the putamen, arteriolosclerosis was as common as in the deep white matter, while venular lesions were relatively rare in some cases. When patients were divided into mild and severe groups according to the median of total arteriolosclerosis or venular collagenosis burden, the severity of arteriolosclerosis significantly increased with venular collagenosis in every brain region, although 20%–30% of the cases still had severe arteriolosclerosis and mild venular collagenosis simultaneously or vice versa (online supplemental table 3). We also found that the severity of venular collagenosis was significantly associated across the brain regions, whereas the severity of arteriolosclerosis was not balanced between the white matter and cortex. Arteriolosclerosis increased synchronously in the white matter and putamen (online supplemental figure 2).

#### Associations of arteriolosclerosis and venular collagenosis with age

The severity of arteriolosclerosis and venular collagenosis significantly increased with age in all brain regions except the putamen, where venular collagenosis was not significantly associated with age (online supplemental figure 3).

#### Associations of arteriolosclerosis and venular collagenosis with parenchymal damage

Associations between arteriolosclerosis and venular collagenosis with each type of parenchymal lesion were assessed in every brain region ([table 2](#)). Compared with those without lacunes, those with lacunes had an increased proportion of arteriolosclerosis only in the putamen ( $p=0.004$ ) but not in other regions, whereas no difference in venular collagenosis was found in any region ( $p>0.1$  for all comparisons). In the hippocampus, venular collagenosis was significantly more common in the microinfarcts group than in the non-microinfarcts group in the hippocampus ( $p=0.036$ ); however, in other regions, both arteriolosclerosis and venular collagenosis were not statistically different between two groups. No association between the degree of myelin loss and arteriolosclerosis was observed in both the periventricular

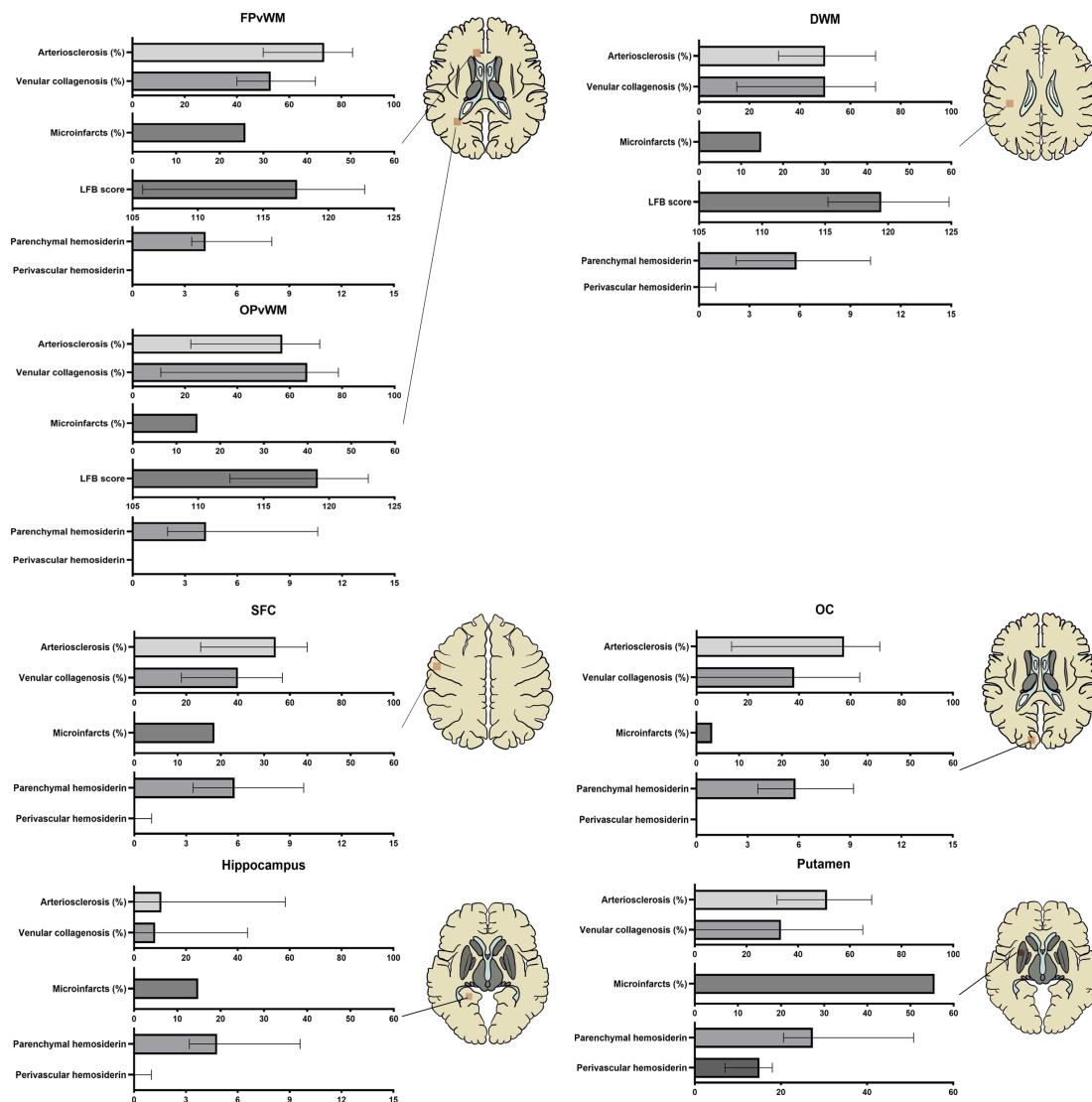


**Figure 2** Parenchymal damages and microvascular wall pathology in different brain regions. Arteriosclerosis (%) =  $\frac{\text{number of sclerotic arterioles}}{\text{total number of arterioles per region}} \times 100\%$ ; venular collagenosis (%) =  $\frac{\text{number of affected venules}}{\text{total number of venules per region}} \times 100\%$ ; perivascular haemosiderin leakage was calculated as the number of affected vessels, and parenchymal haemosiderin deposits were calculated as the average number of haemosiderin spots per area ( $4 \text{ mm}^2$ ). DWM, deep white matter of parietal lobe; FPvWM, frontal periventricular white matter; LFB, luxol fast blue (represent the severity of myelin loss); OC, occipital cortex OPvWM, occipital periventricular white matter; SFC, superior frontal cortex.

and deep white matter; however, lower white matter pallor values (indicating myelin loss) were significantly associated with an increased proportion of venular collagenosis in these regions. After adjusting for age, venular collagenosis was still associated with white matter pallor in the occipital periventricular white matter ( $r=-0.469$ ,  $p=0.016$ ) and deep white matter ( $r=-0.437$ ,  $p=0.025$ ) but not in the frontal periventricular white matter ( $r=-0.344$ ,  $p=0.086$ ). Neither arteriosclerosis nor venular collagenosis was associated with perivascular or brain parenchymal haemosiderin deposits in any region ( $p>0.1$  for all comparisons, online supplemental table 3), except in the superior frontal cortex, where arteriosclerosis correlated with decreased brain parenchymal haemosiderin deposits ( $p=0.024$ ).

## DISCUSSION

In this study, we demonstrated that arteriosclerosis and venular collagenosis were significantly correlated with age and were commonly observed in the white matter regions. More severe myelin loss was significantly associated with increased collagenised venules but not sclerotic arterioles, whereas lacunes were only associated with more severe arteriosclerosis in the putamen but not with venular collagenosis in any region. Neither of these microvascular pathologies was associated with perivascular or parenchymal haemosiderin. Our results indicate that arteriosclerosis and venular collagenosis may be involved in the different subtypes of parenchymal damage.

**Table 2** Associations of parenchymal lesions with vascular pathology

	Lacunes in gross specimen†			Microinfarct‡			Myelin loss‡			Haemosiderin‡		
	Present n=16	Absent n=9	P value	Present n=18	Absent n=9	P value	β	P value	β	P value	β	P value
Arteriosclerosis (%)§ in brain regions												
FPvWM	77.4, 50.9–84.4	64.3, 36.4–79.2	0.257	79.6, 62.5–85.7	61.9, 46.–76.5	0.091	-0.078	0.703	0.515	0.007	0.173	0.399
OPvWM	58.5, 22.0–76.7	52.9, 23.5–56.4	0.332	62.3, 23.5–75.9	53.6, 22.2–57.9	0.201	-0.036	0.862	0.220	0.281	0.020	0.921
DWM	42.7, 34.0–73.9	50.0, 25.0–55.3	0.558	52.6, 31.6–78.6	40.0, 33.3–50.0	0.184	-0.243	0.232	0.082	0.691	-0.214	0.295
SFC	56.4, 28.0–70.8	41.2, 19.2–60.0	0.292	59.2, 37.5–67.6	40.0, 19.2–66.7	0.337	-	-	0.182	0.373	-0.440	0.024*
OC	61.8, 26.9–81.7	16.7, 0–65.2	0.138	59.4, 13.6–78.3	42.8, 23.1–66.7	0.721	-	-	-0.059	0.773	0.097	0.638
Hippocampus	9.8, 0.0–59.2	10.5, 0–50.0	0.954	45.5, 0.0–60.0	8.3, 0.0–10.0	0.114	-	-	-0.232	0.253	-0.019	0.925
Putamen	59.2, 46.4–76.7	30.0, 24.1–40.9	0.004*	53.8, 31.8–68.4	50.0, 40.9–61.5	0.959	-	-	0.028	0.890	0.294	0.144
Venular collagenosis (** in brain regions												
FPvWM	55.4, 36.7–70.0	64.7, 45.5–75.0	0.758	59.7, 46.3–70.0	45.5, 33.3–70.0	0.290	-0.344	0.086	0.054	0.792	0.008	0.971
OPvWM	66.7, 9.2–81.6	53.3, 10.7–66.7	0.373	66.7, 11.8–81.8	57.1, 10.7–75.0	0.683	-0.469	0.016*	0.136	0.507	-0.108	0.598
DWM	51.7, 8.8–69.7	40.0, 22.2–66.7	0.801	54.6, 40.0–70.6	18.2, 0–66.7	0.122	-0.437	0.025*	0.324	0.107	0.090	0.662
SFC	34.5, 28.2–57.7	41.7, 0–57.1	0.778	42.2, 25.5–57.1	35.7, 0–41.6	0.347	-	-	0.327	0.103	-0.167	0.415
OC	31.7, 2.6–67.1	38.1, 0–57.6	0.713	43.7, 0–63.6	33.3, 11.5–63.6	0.837	-	-	-0.096	0.642	-0.034	0.869
Hippocampus	4.1, 0.0–32.1	0.0, 0.0–31.3	0.928	26.5, 0–60.0	0.0, 0.0–0.0	0.036*	-	-	-0.081	0.695	-0.196	0.341
Putamen	34.5, 0.0–58.3	0.0, 0.0–53.8	0.454	33.3, 0–65.0	41.6, 0–53.8	0.855	-	-	-0.073	0.723	-0.256	0.206

\*p<0.05.

†Associations with lacunes and microinfarcts were calculated using Wilcoxon signed-rank test (by defining microinfarct-mild/microinfarct-severe groups and lacunes/non-lacunes groups per region), and there was no significant difference in age at death between groups.

‡Associations with white matter pallor, perivascular haemosiderin leakage and parenchymal haemosiderin deposits were calculated using Spearman correlation test, adjusted for age.

§Arteriosclerosis (%) =  $\frac{\text{number of sclerotic arterioles}}{\text{total number of arterioles per region}} \times 100\%$ .

\*\*Venular collagenosis (%) =  $\frac{\text{number of affected venules}}{\text{total number of venules per region}} \times 100\%$ .

DWM, deep white matter of parietal lobe; FPvWM, frontal periventricular white matter; OC, occipital cortex; OPvWM, occipital periventricular white matter; SFC, superior frontal cortex.

Unlike arterioles, cerebral venules have been consistently ignored in neuropathological studies. This is owing to the limited number of histological methods for identifying cerebral venules. The method of anti- $\alpha$ SMA immunohistochemical staining, which relies on the continuous wreath of concentric smooth muscle in the arteries, has been commonly used in previous pathological studies.<sup>5</sup> However, arterioles may be misinterpreted as venules when arteriolosclerosis occurs because of smooth muscle cell loss and fibrohyalinised material deposits.<sup>6,10</sup> Anti-MCT1 immunohistochemical staining, a sensitive and reliable method for distinguishing cerebral venules from arterioles, combined with anti- $\alpha$ SMA, was used in our study to overcome these problems.<sup>8</sup>

We found that although the severity of arteriolosclerosis significantly increased with venular collagenosis across the brain regions, an inverse severity distribution was found in 20%–30% of cases. These data suggest that, despite some shared risk factors, the mechanisms underlying the development of arteriolosclerosis and venous collagenosis might differ. Additionally, more severe sclerotic arterioles were distributed in the white matter and putamen than in the cortex, which is in line with previous knowledge. However, the burden of collagenised venules in all the brain regions was balanced. In recent brain venule studies using MRI, most researchers visually counted only deep medullary veins of regular arrangement perpendicular to the ventricles. Our findings suggest

that venular lesions in one brain region can represent those of the whole brain.

Arteriolosclerosis has been commonly recognised as a critical cause of leukoaraiosis, while recent pathological studies on collagenised veins/venules have also suggested a close relationship with white matter pallor.<sup>4,5</sup> In this study, our findings challenge the widely accepted knowledge that arteriolosclerosis is the main vascular cause of leukoaraiosis. A potential explanation might be that collagenised venules could be misinterpreted as sclerotic arterioles by the common staining methods of anti- $\alpha$ SMA immunohistochemical staining and Masson's trichrome staining (figure 3), which has also attracted the attention of researchers in previous studies.<sup>6</sup> Our findings further support the important role of venules in aggravating white matter lesions.<sup>4</sup> Narrowed venules accompanied by increased pressure and vascular resistance can result in blood–brain barrier leakage and exudation of fluid into interstitial spaces, leading to vasogenic oedema.<sup>6</sup> Interstitial oedema impairs the neuropil nearby, aggravating demyelination and gliosis.<sup>4</sup> The impaired white matter could also stimulate venular collagen deposition in response to weak mechanical support of the vessels.<sup>11</sup>

It is not surprising that lacunes are more likely to be associated with arteriolar diseases rather than venular diseases because arteriolosclerosis might result in occlusion of the supplying artery and complete

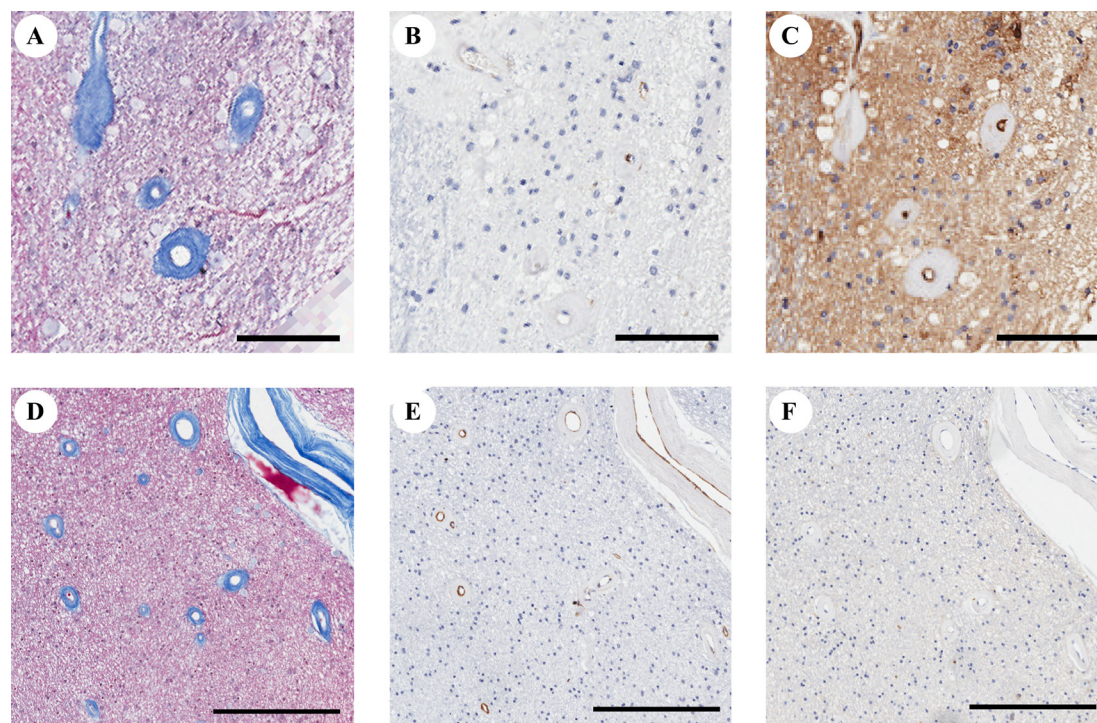


**Figure 3** An example of confounding microvascular types. The microvascular walls on Masson's trichrome-stained image (A, occipital periventricular white matter from patient 27, and (D), frontal periventricular white matter from patient 27) are quite the same. Both of them have a thin anti- $\alpha$ SMA stained pattern (B, E). The microvessel with positive immunolabeled for MCT1 (C) is considered as venules, and other microvessels with negative immunolabeled for MCT1 (F) are considered as arterioles. Bar=100  $\mu$ m for A–C, and bar=300  $\mu$ m for D–F.  $\alpha$ SMA, alpha-smooth muscular actin.



ischaemia as a consequence.<sup>12</sup> In general, the lack of association between microvascular wall pathologies and brain haemosiderin deposits found in our study is inconsistent with previous reports.<sup>13</sup> This might be related to the differences in the study population. Previous studies mainly investigated patients with cerebral amyloid angiopathy and found that small vessels could be involved in vascular amyloid-beta accumulation to aggravate the progression of haemosiderin deposits in vascular walls.<sup>13</sup> In contrast, for the aged donors in our study, haemosiderin was much less common, which might limit the statistical power.

Our findings imply different roles for arteriosclerosis and venular collagenosis in relation to different subtypes of microvessel-related parenchymal damage, which may have been previously overlooked. The anatomical branching patterns,<sup>14</sup> tortuosity<sup>15</sup> and age-related pathologies<sup>16</sup> differ significantly depending on the vessel type (arteriolar or venular). In particular, arterioles are the primary site of vascular resistance, where the greatest changes in blood pressure and flow velocity occur.<sup>17</sup> The physiological function of the arterial system mainly includes blood and nutrient supply, and that of venules includes material exchange, inflammatory cell infiltration and fluid drainage.<sup>16</sup> Hence, it is not challenging to understand the pathological changes in arterioles or venules that might result in different brain parenchymal lesions.

The main limitation of our study is its small sample size. As in common pathological studies, the selected samples in our observational study could not represent the whole-brain status, although multiple regions were assessed. Second, although cases with stroke or brain tumour history were ruled out, the heterogeneous disease background of the samples can not be ignored. In addition, the information on risk factors and neuroimaging is crucial; however, the small sample size, incomplete premortem data and lack of postmortem imaging data hindered the further analysis of potential factors of arteriosclerosis and venular collagenosis.

In summary, our study highlights the importance of cerebral small venous disease in vascular parenchymal lesions. Further studies on brain arterioles and venules are warranted to improve our understanding of the heterogeneity of cerebral small vessel diseases.

#### Author affiliations

<sup>1</sup>Department of Neurology, State Key Laboratory of Complex Severe and Rare Diseases, Peking Union Medical College Hospital, Chinese Academy of Medical Sciences and Peking Union Medical College, Beijing, China

<sup>2</sup>Department of Human Anatomy, Histology and Embryology, Institute of Basic Medical Sciences, Neuroscience Center, Chinese Academy of Medical Sciences, School of Basic Medicine, Peking Union Medical College, Beijing, China

**Contributors** YC: conceptualisation, investigation, formal analysis, writing—original draft, visualisation. M-YH: investigation, formal analysis, writing—original draft, visualisation. Y-CZ: conceptualisation, supervision, writing—review and editing, funding acquisition, guarantor. W-YQ: methodology, investigation, writing—review and editing. C-HM, XW, Y-YX and X-JQ: formal analysis, software, writing—review and editing. CM: conceptualisation, supervision.

**Funding** This work was supported by the National Natural Science Foundation of China (No. 81971138), the Chinese Academy of Medical Sciences Innovation Fund for Medical Sciences (CIFMS 2021-I2M-1-025), the Strategic Priority Research Program 'Biological basis of aging and therapeutic strategies' of the Chinese Academy of Sciences (XDB39040300), and the Science Innovation 2030-Brain Science and Brain-Inspired Intelligence Technology Major Project (No. 2021ZD0201100) Task 5 (No. 2021ZD0201105).

**Competing interests** None declared.

**Patient consent for publication** Not applicable.

**Ethics approval** This study involves human participants and was approved by the Institutional Review Board of the Institute of Basic Medical Sciences of the Chinese Academy of Medical Sciences/Peking Union Medical College, Beijing, China (approval number: 009-2014). Participants gave informed consent to participate in the study before taking part.

**Provenance and peer review** Not commissioned; externally peer reviewed.

**Data availability statement** All data relevant to the study are included in the article or uploaded as online supplemental information.

**Supplemental material** This content has been supplied by the author(s). It has not been vetted by BMJ Publishing Group Limited (BMJ) and may not have been peer-reviewed. Any opinions or recommendations discussed are solely those of the author(s) and are not endorsed by BMJ. BMJ disclaims all liability and responsibility arising from any reliance placed on the content. Where the content includes any translated material, BMJ does not warrant the accuracy and reliability of the translations (including but not limited to local regulations, clinical guidelines, terminology, drug names and drug dosages), and is not responsible for any error and/or omissions arising from translation and adaptation or otherwise.

**Open access** This is an open access article distributed in accordance with the Creative Commons Attribution Non Commercial (CC BY-NC 4.0) license, which permits others to distribute, remix, adapt, build upon this work non-commercially, and license their derivative works on different terms, provided the original work is properly cited, appropriate credit is given, any changes made indicated, and the use is non-commercial. See: <http://creativecommons.org/licenses/by-nc/4.0/>.

#### ORCID iDs

Yuan Cao <http://orcid.org/0000-0003-4257-6908>

Mei-Ying Huang <http://orcid.org/0000-0002-5031-7423>

Yi-Cheng Zhu <http://orcid.org/0000-0002-8966-1379>

#### REFERENCES

- Montine TJ, Phelps CH, Beach TG, *et al.* National Institute on Aging-Alzheimer's association guidelines for the neuropathologic assessment of Alzheimer's disease: a practical approach. *Acta Neuropathol* 2012;123:1–11.
- Skrobot OA, Attens J, Esiri M, *et al.* Vascular cognitive impairment neuropathology guidelines (VCING): the contribution of cerebrovascular pathology to cognitive impairment. *Brain* 2016;139:2957–69.
- Kövari E, Herrmann FR, Gold G, *et al.* Association of cortical microinfarcts and cerebral small vessel pathology in the ageing brain. *Neuropathol Appl Neurobiol* 2017;43:505–13.
- Moody DM, Brown WR, Challa VR, *et al.* Periventricular venous collagenosis: association with leukoariosis. *Radiology* 1995;194:469–76.
- Keith J, Gao F-Q, Noor R, *et al.* Collagenosis of the deep medullary veins: an underrecognized pathologic correlate of white matter hyperintensities and periventricular infarction? *J Neuropathol Exp Neurol* 2017;76:299–312.
- Petersen JA, Keith J, Gao F, *et al.* Cadasil accelerated by acute hypotension: arterial and venous contribution to leukoariosis. *Neurology* 2017;88:1077–80.
- Qiu W, Zhang H, Bao A, *et al.* Standardized operational protocol for human brain banking in China. *Neurosci Bull* 2019;35:270–6.
- Cao Y, Ao D-H, Ma C, *et al.* Immunoreactivity and a new staining method of monocarboxylate transporter 1 located in endothelial cells of cerebral vessels of human brain in distinguishing cerebral venules from arterioles. *European Journal of Histochemistry* 2021;65.
- Deramecourt V, Slade JY, Oakley AE, *et al.* Staging and natural history of cerebrovascular pathology in dementia. *Neurology* 2012;78:1043–50.
- Pantoni L. Cerebral small vessel disease: from pathogenesis and clinical characteristics to therapeutic challenges. *Lancet Neurol* 2010;9:689–701.



- 11 Henry-Feugeas MC, Koskas P. Cerebral vascular aging: extending the concept of pulse wave encephalopathy through capillaries to the cerebral veins. *Curr Aging Sci* 2012;5:157–67.
- 12 Brown WR, Moody DM, Challa VR, *et al.* Venous collagenosis and arteriolar tortuosity in leukoaraiosis. *J Neurol Sci* 2002;203–204:159–63.
- 13 Gurol ME, Dierksen G, Betensky R, *et al.* Predicting sites of new hemorrhage with amyloid imaging in cerebral amyloid angiopathy. *Neurology* 2012;79:320–6.
- 14 Cassot F, Lauwers F, Lorthois S, *et al.* Branching patterns for arterioles and venules of the human cerebral cortex. *Brain Res* 2010;1313:62–78.
- 15 Lorthois S, Lauwers F, Cassot F. Tortuosity and other vessel attributes for arterioles and venules of the human cerebral cortex. *Microvasc Res* 2014;91:99–109.
- 16 Brown WR, Thore CR. Review: cerebral microvascular pathology in ageing and neurodegeneration. *Neuropathol Appl Neurobiol* 2011;37:56–74.
- 17 Blevins BL, Vinters HV, Love S, *et al.* Brain arteriolosclerosis. *Acta Neuropathol* 2021;141:1–24.